A COMPACT OPTICAL PULSE COMPRESSOR WITH
COMPUTER-GENERATED HOLOGRAPHIC MASKS FOR RADAR
APPLICATIONS(U) NAVAL RESEARCH LAB WASHINGTON DC
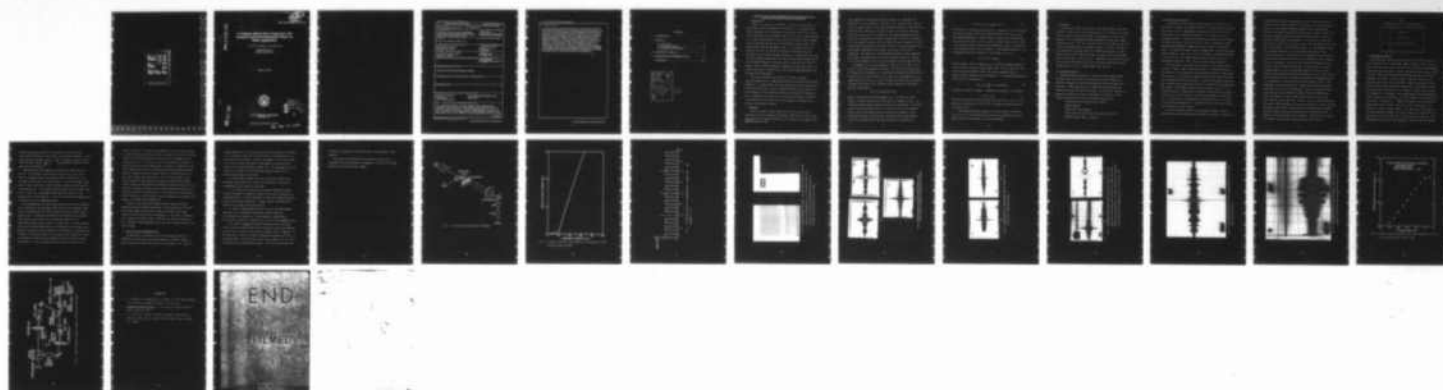S C LIN ET AL. 24 AUG 83 NRL-MR-5134   F/G 17/9   NL

UNCLASSIFIED

MICROCOPY RESOLUTION TEST CHART
NATIONAL BUREAU OF STANDARDS-1963-A

A Compact Optical Pulse Compressor with Computer-Generated Holographic Masks for Radar Applications

S. C. LIN, R. A. ATHALE, AND JOHN N. LEE

Applied Optics Branch
Optical Sciences Division

August 24, 1983

DTIC
ELECTE
SEP 7 1983

D

NAVAL RESEARCH LABORATORY
Washington, D.C.

83 09 07 030

REPORT DOCUMENTATION PAGE		READ INSTRUCTIONS BEFORE COMPLETING FORM
1. REPORT NUMBER NRL Memorandum Report 5134	2. GOVT ACCESSION NO. AD-A132152	3. RECIPIENT'S CATALOG NUMBER
4. TITLE (and Subtitle) A COMPACT OPTICAL PULSE COMPRESSOR WITH COMPUTER-GENERATED HOLOGRAPHIC MASKS FOR RADAR APPLICATIONS		5. TYPE OF REPORT & PERIOD COVERED Progress report 23 Apr 1982 — 30 Sept 1982
		6. PERFORMING ORG. REPORT NUMBER
7. AUTHOR(s) S.C. Lin, R.A. Athale and John N. Lee		8. CONTRACT OR GRANT NUMBER(s)
9. PERFORMING ORGANIZATION NAME AND ADDRESS Naval Research Laboratory Washington, DC 20375		10. PROGRAM ELEMENT, PROJECT, TASK AREA & WORK UNIT NUMBERS 64352N; 50179-AA; 65-1686-0-2
11. CONTROLLING OFFICE NAME AND ADDRESS Naval Surface Weapons Center Dahlgren, VA 22448		12. REPORT DATE August 24, 1983
		13. NUMBER OF PAGES 26
14. MONITORING AGENCY NAME & ADDRESS(if different from Controlling Office)		15. SECURITY CLASS. (of this report) UNCLASSIFIED
		15a. DECLASSIFICATION/DOWNGRADING SCHEDULE

16. DISTRIBUTION STATEMENT (of this Report)

Approved for public release; distribution unlimited.

17. DISTRIBUTION STATEMENT (of the abstract entered in Block 20, if different from Report)

18. SUPPLEMENTARY NOTES

19. KEY WORDS (Continue on reverse side if necessary and identify by block number)

Radar pulse compression
Acoustooptics
Laser diode light source

Computer-generated holographic masks
Binary codes

20. ABSTRACT (Continue on reverse side if necessary and identify by block number)

A compact acoustooptical (A-O) pulse compressor using computer-generated holographic masks to generate and to match-filter the return pulses has been demonstrated to be suitable for radar use. The basic working principle of the system is given. Descriptions of the A-O Bragg cell, the computer generated holographic masks, carrying 4-bit, 7-bit, and 13-bit Barker codes and pseudorandom codes up to a length

(Continues)

DD FORM 1473 EDITION OF 1 NOV 55 IS OBSOLETE
1 JAN 73
S/N 0102-014-6601

20. ABSTRACT (Continued)

of 511 bits, and the unique use of a diode laser as the light source are given. Experimental results are given for all the Barker codes and pseudorandom codes up to 127 bits. The results showed very good agreement with the theoretical predictions. For codes longer than 127 bits, it was found that a longer, high-quality acoustooptical interaction region in the Bragg cell must be obtained to ensure better correlation. This can be done through crystal selection and transducer apodization. The dynamic range of the system is 40 dB with high linearity at 7 mW of diode laser output. Finally, specific areas, which are important to the enhancement of the system versatility and agility, are recommended for future work. These are; (i) multichannel device for agility, (ii) ECL digital storage units for preprogrammed waveforms and for generating time-reversed reference waveforms, (iii) Doppler shift cancellation and Doppler shift scanning, and (iv) system miniaturization and ruggedization.

CONTENTS

iii

A COMPACT OPTICAL PULSE COMPRESSOR WITH COMPUTER-GENERATED HOLOGRAPHIC MASKS FOR RADAR APPLICATIONS

I. INTRODUCTION

A means for increasing the capability of an existing radar system is to simply employ larger time-bandwidth (TBW) waveforms. Such waveforms can provide advantages such as elimination of distributed clutter (e.g., rain), better range resolution and detection capability at a given transmitter power (i.e., high pulse-compression ratio), and better protection against jammers. With such waveforms one requires a pulse compressor (matched filter) with commensurately large TBW and dynamic range. It is desirable that such a processor be able to be retrofitted into existing systems and satisfy constraints on size, weight and power consumption. An additional factor that can affect hardware implementation is that with large TBW waveforms matching of the reference waveform to the radar return is especially critical; for example, unless a reference waveform is generated for each radar return on a pulse-by-pulse basis, instabilities in the reference waveform generator can adversely affect performance.

This report describes initial results of an effort to employ recently-developed optical technology to perform pulse compression and pulse generation in a compact module that can be applied to existing systems such as the Mk92 and Mk86 radars. Optical techniques have been used previously for pulse compression,[1] but performance problems have limited their systems use. Also, no attempt has been made to use a single optical system for producing the transmitted pulses as well as for pulse compression, although such a concept is theoretically feasible.

II. APPROACH

The pulse compressor demonstrated here utilized the latest optical technology available: high-power semiconductor diode lasers as light sources, high-diffraction-efficiency acousto-optic (A-O) Bragg cells for signal input,

1

computer-generated holograms for reference waveforms, and high-speed PIN
photodiodes for signal detection. The small size of the diode lasers opens up
a door for compact design; the efficient high-power operation, coupled with the
high diffraction efficiency of the A-O cell would give a dynamic range only
limited by the saturation of the detector. The computer-generated waveforms
offer the first opportunity to control the phase error to within a few degrees,
and a large number of masks of different codes can be easily produced for both
encoding the transmitted pulses and match-filtering. High-speed detectors with
large dynamic range enable one to adapt to any relevant radar carrier
frequencies. The combination of above advantages offered by these components
and a design for ruggedization of the optical assembly results in a compact
optical pulse compressor that is not only versatile, but also power-efficient.

The schematic of the pulse compressor is given in Fig. 1, which can be
used to illustrate the operating principles. The light from the diode laser,
of frequency ω_ℓ and wavelength λ, is collimated and transmitted through the A-O
Bragg cell which is being driven by an rf signal $A(t) \cos\omega_a$ where $A(t)$ is the
complex amplitude of the input signal. The amplitude of the light diffracted by
the Bragg cell contains the amplitude and phase information on the acoustic
wave and is described by

$$A(t- \frac{z}{v}) \cos [\omega_\ell t + \omega_a(t-z/v)] \qquad (1)$$

where z is the position along the Bragg cell and v is the acoustic wave
velocity. Note the Doppler shift of the light to a frequency $(\omega_\ell + \omega_a)$. The
diffracted light undergoes a second diffraction by the hologram. The hologram
contains the reference waveform $B(-z)$ on a spatial carrier with wavelength
equal to that of the acoustic wave (Λ_0) at the center frequency. Hence,
the doubly-diffracted light beam after the hologram travels approximately
parallel to the undiffracted light beam direction and is described by

2

$$A(t- \frac{z}{v}) \, B(-z) \cos\left[\omega_\ell t + \omega_a (t-z/v)\right] \qquad (2)$$

The direction of the doubly-diffracted light is important; a lens now focusses both the undiffracted light and the doubly-diffracted light onto a single, high-speed photodetector. Coherent detection results, with the undiffracted light serving as the local oscillator source. Coherent detection will result in much greater dynamic range, since the photodetector output is proportional to the amplitude, rather than the intensity, of the signal-bearing beam. The photodetector output for a given light ray as shown in Fig. 1 is

$$A(t - \frac{z}{v}) \, B(-z) \cos(\omega_a t) \qquad (3)$$

Note the temporal carrier frequency ω_a, the difference frequency between the local-oscillator and signal-carrying light beams. The lens focuses all rays within the window defined by the A-O cell and the hologram, giving an effective signal integration over the window (L). The resultant photodetector output current is proportional to

$$I(t) \propto \int_L A(t \, \frac{z}{v} -) \, B(-z) \cos(\omega_a t)dz, \qquad (4)$$

the desired correlation integral. A matched filter operation is achieved if

$$B(-z) = A(-z) \qquad (5)$$

Note that the sense of B must be reversed from that of $A(t)$. Also, if $A(t)$ is made to be a delta function, $\delta(t)$, Eq. (4) represents the signal encoded on the hologram, $B(-t)$.

In the demonstrated pulse compressor, the total length of the optical train is 35 cm. The next subsections describe the requirements and choices made for each of the components in the pulse compressor.

II.1 Diode Lasers

Maximum optical power is required for good dynamic range. Single mode operation is required for coherent detection and for uniformity of the optical intensity across the processing window. A long operating lifetime is also essential. For the demonstrated system a Mitsubishi TJS-type laser (Model ML-5308) was chosen. This laser provides 15 mW of optical power at 823 nm at 70 mA drive current and has a projected lifetime of 10^6 hours. The laser is best operated with a battery source and in continuous operation, as large power transients lead to reduced lifetime. A typical curve of light output versus drive current is shown in Fig. 2. Subsequent to this particular choice of laser, even higher power lasers with the required characteristics have become available, such as a 40-mW LOC-type laser from RCA.

II.2 Acousto-optic Bragg cell

Maximum diffraction efficiency is required for good dynamic range. Slow-shear-mode TeO_2 was chosen as providing an optimum combination of bandwidth, reasonably low acoustic-wave attenuation and high diffraction efficiency. (Other materials such as $LiNbO_3$ have better bandwidth and attenuation but poor diffraction efficiency.) The Bragg cell required is commercially available from several manufacturers; the actual cell was obtained from Harris Corp. with the following characteristics.

> 12% diffraction efficiency/rf watt at 850 nm
>
> 50 MHz bandwidth
>
> 80 MHz center band frequency
>
> 10 μsec aperture used, 50 μsec total aperture available
>
> Maximum rf power input of 1 watt cw

4

II.3 Computer-Generated Hologram

The acoustooptic pulse compressor design studied in this report uses a fixed mask to represent the reference waveform. Since the reference waveforms most commonly used are phase-modulated codes and an ordinary mask can only encode positive real transmittance functions, it is necessary to go to a holographic approach. Although analog volume phase hologram have the highest diffraction efficiency, they are difficult to control and generate. Binary-amplitude, computer-generated holograms were therefore chosen for the present system. The reference waveforms chosen for demonstration purposes were Barker codes of lengths 4, 7, and 13 bits, and direct sequence, spread-spectrum codes 31, 63 and 127 bits long. These reference waveforms simply consist of a predetermined pattern of 0 and π phase shifts with constant amplitude.

The phase shifts in the codes can be encoded by using a spatial carrier frequency. Figure 3 shows the amplitude profile of a hologram that uses a binary spatial carrier frequency to encode the given pattern of 0 and π phase shift pattern. In this particular example the binary grating has a 50% duty cycle for maximum diffraction efficiency. To satisfy the sampling theorem one must include at least one period of the carrier in one bit of the binary phase data stream. In the example shown we have three periods in one bit. The transition from 0 to π phase shift is achieved by shifting the binary grating in the next bit to the right by half a period and conversely the transition from π to 0 phase shift is accomplished by shifting the grating in the next bit to the left (thereby making it in phase with other bits carrying 0 phase shift information) by half a period.

The carrier frequency grating of the holographic reference waveform serves another purpose besides encoding the phase information. Since we use a

5

coherent detection scheme to increase dynamic range, the optical beam that is multiplied by the input waveform (via the Bragg cell) and the reference waveform (via the computer generated hologram) should be approximately parallel to the undiffracted beam which serves as the local oscillator. So the carrier frequency grating must provide a deflection that is equal but opposite to that imposed by the Bragg cell. This condition is met if the spatial period of the carrier grating is equal to the wavelength of the sound wave in TeO_2 crystal at the RF center frequency. For the parameters chosen for the demonstration this is 8 μm, thus making the linewidth 4 μm. In order to ensure very low distortions in the sidelobes of the correlation output, phase noises associated with the pulse compressor must be controlled to within a few degrees. Thus puts a very stringent requirement on the accuracy of setting the grating spacings. This performance can be easily achieved, however, by using the E-beam mask generation facility in the Microelectronics Fabrication Section at NRL because it has a 0.1 μm resolution and 100 Å setting accuracy. An electron beam exposes the photoresist layer on a chrome-plated, ultra-flat glass plate under computer control. After development, the exposed photoresist is washed away uncovering underlying chrome layer which can then be etched away. We can thus obtain the desired chrome pattern on a glass blank as dictated by the data provided to the controlling computer. Figure 4 shows a magnified portion of a 511 bit direct-sequence, binary phase code. The 0 to π and π to 0 phase transitions can be easily identified based on the previous explanation. Table I shows the three Barker code reference waveforms used in the demonstration experiment. The direct sequence codes were calculated using different-length shift registers and using different taps for feedback. The description of these shift register codes and their properties can be found in Ref. 2.

6

TABLE I

Barker Codes with 4, 7, 13 bits lengths.

4	$0\ 0\ \pi\ 0$
7	$0\ 0\ 0\ \pi\ \pi\ 0\ \pi$
13	$0\ 0\ 0\ 0\ 0\ \pi\ \pi\ \pi\ 0\ 0\ \pi\ 0\ \pi$

III. EXPERIMENTAL RESULTS

Experiments were carried out for the Barker codes of 4-bit, 7-bit, and 13-bit lengths and for the pseudorandom codes of lengths 31 and 64 bits. We first used a He-Ne laser as the light source for the optical pulse compressor, knowing the high-quality beam it outputs. Results are shown in Figs. 5 and 6. Figure 5(a) shows the correlation of the 4-bit Barker code. The RF pulse, phase-coded as in Table 1, is about 10 μsec in duration, giving rise to a correlation trace about twice the duration. Figure 5(b) and 5(c) are 7-bit and 13-bit Barker codes correlations, respectively. The compressed central peak width, which is proportional to bit length, is clearly seen to decrease the as number of bits increases. The sidelobe patterns show good agreement with the theoretical calculations. The slight asymmetry is due mainly to the distortions in the Bragg cell. Similarly, correlations of 31-bit and 63-bit pseudo-random codes are shown in Fig. 6(a) and 6(b), respectively. The compression is seen to be more dramatic. The distortions of the Bragg cell also has an effect on the sidelobes. The peak-to-sidelobe ratio does not follow the theoretical value of 1/N, where N is the length of the code used. One reason may be the distortions just mentioned. The other intrinsic reason is

7

that the codes we used, especially those encoded on the masks, are of single length, resulting in finite-length, single-frame correlations. In this case, the known theoretical value is $1/\sqrt{N}$. For example, instead of 1/63 in the 63-bit case, we have $\dfrac{1}{\sqrt{63}} \approx \dfrac{1}{8}$. The experimental result of Fig. 6(b) agrees with the estimation.

Experiments were then repeated by using the diode laser described in Sec. 2.1. This allowed a large reduction in size in the light source. Results of comparable quality have been achieved. We show in Fig. 7 the correlation of 4-bit and 7-bit Barker codes. In Fig. 7(a), the upper trace shows a single coded RF pulse, while the lower one shows the correlation of the coded wave form. The correlation shows the doubling of the length of the pulse. In Fig. 7(b), the asymmetry again shows the distortion in the particular part of the Bragg cell. In Fig. 8, we show the high compression of the pulse for a 127-bit pseudorandom code.

We also demonstrated the code readout capability of our pulse compressor. This is pertinent to the requirement that the code of the transmitted radar pulse is self-generated. One typical readout of the 13-bit Barker code is shown in Fig. 9. The upper trace shows, on its lefthand side, a simulated delta function required for such a time-reversing operation. The time-reversed readout pulse is shown in the lower trace. The delay from the first-bit to the feed-through pulse on the lefthand side of the lower trace measures the distance from the transducer of the Bragg cell to the edge of the hologram. The non-uniform height in the envelope of the readout code is due to the Bragg cell distortion which produced a nonuniform diffracted-light distribution. In fact, the Bragg cell we used was not selected for its

8

optical uniformity. The acoustic wave generated in the cell does not produce a uniform grating across the cell aperture. One may also note that the finite length of the simulated delta-pulse can give rise, to some degree, to the distortion as well. As a result, out of a 50 µsec window only a section of about 10 µsec can be used to produce good correlations. The 255-bit and the 511-bit codes did not allow us to obtain good correlations because the code lengths in the masks exceed the length in the cell corresponding to the 10 µsec time. However, the nonuniformity is not an intrinsic defect in the system, because the usable section of window can be much improved through careful selection of the TeO_2 crystal and amplitude weighting function for the Bragg cell transducer to produce a more uniform acoustic wave distribution in the axial direction[3]. Sharpe pulses of ~ 4 nsec duration can also be used for better simulation of a delta function (such pulse generator are available, for example, from AVTECH Electro-Systems Ltd.).

Finally, we have measured the dynamic range of the existing pulse compressor based on the peak-to-peak height of the correlation of the 4-bit Barker code, because this was the case where the correlation was least distorted by phase nonuniformity of the Bragg cell. The result is plotted in Fig. 10 against the RF power level , maintaining the diode laser output at 7mW. The dynamic range was observed to be linear over a region of 40 dB in the input RF power.

IV. CONCLUSION AND RECOMMENDATIONS

The experimental investigation so far have demonstrated that pulse compression can be achieved with computer-generated, holographic masks for practical Barker and pseudo-random codes up to bit-length of 127. Codes of

9

lengths exceeding 127 bits can be used when the useful aperture of the Bragg cell is increased by improving the optical quality of the TeO_2 crystal and apodization of the transducer. With this improvement, a full 50 µsec window can be used to increase the number of code lengths for each correlation operation to increase the peak-to-sidelobe ratio. The improvement would also restore to full capability the code readout operation through which a self-contained system can be ensured.

The linear dynamic range has been found to be 40 dB. Based on the performance established so far for the pulse compressor, the following recommendations can be made for future work:

(a) To enhance the versatility of the system, multichannel devices should be developed for addressable readout of the codes for encoding the transmitted pulses. The same coded masks or identically reproduced ones can then be used for pulse compression. To ensure agility, the switching of channels must be done quickly and accurately.

(b) Digital storage systems can also be used to store preprogrammed waveforms, and for generating time-reversed reference waveforms, but they must be ECL compatible. In this approach, a second Bragg cell may also be used as a matched filter, in lieu of the holographic mask.

(c) In order to compensate the effect of Doppler shift in the radar return, one may use the well-known linear FM waveform, because this waveform give rise to a correlation least sensitive to Doppler shift in frequency. On the other hand, it may be of interest to determine the Doppler shift due to the target motion. Then techniques, such as the one shown in Fig. 11, can be devised in the pulse compression correlator. The precise configuration that

10

is amenable to retrofitting into existing radar systems requires further attention.

(d) Finally, the miniaturization of the physical size and the ruggedization of the system should be addressed in the light of the space limitation in the existing radar systems.
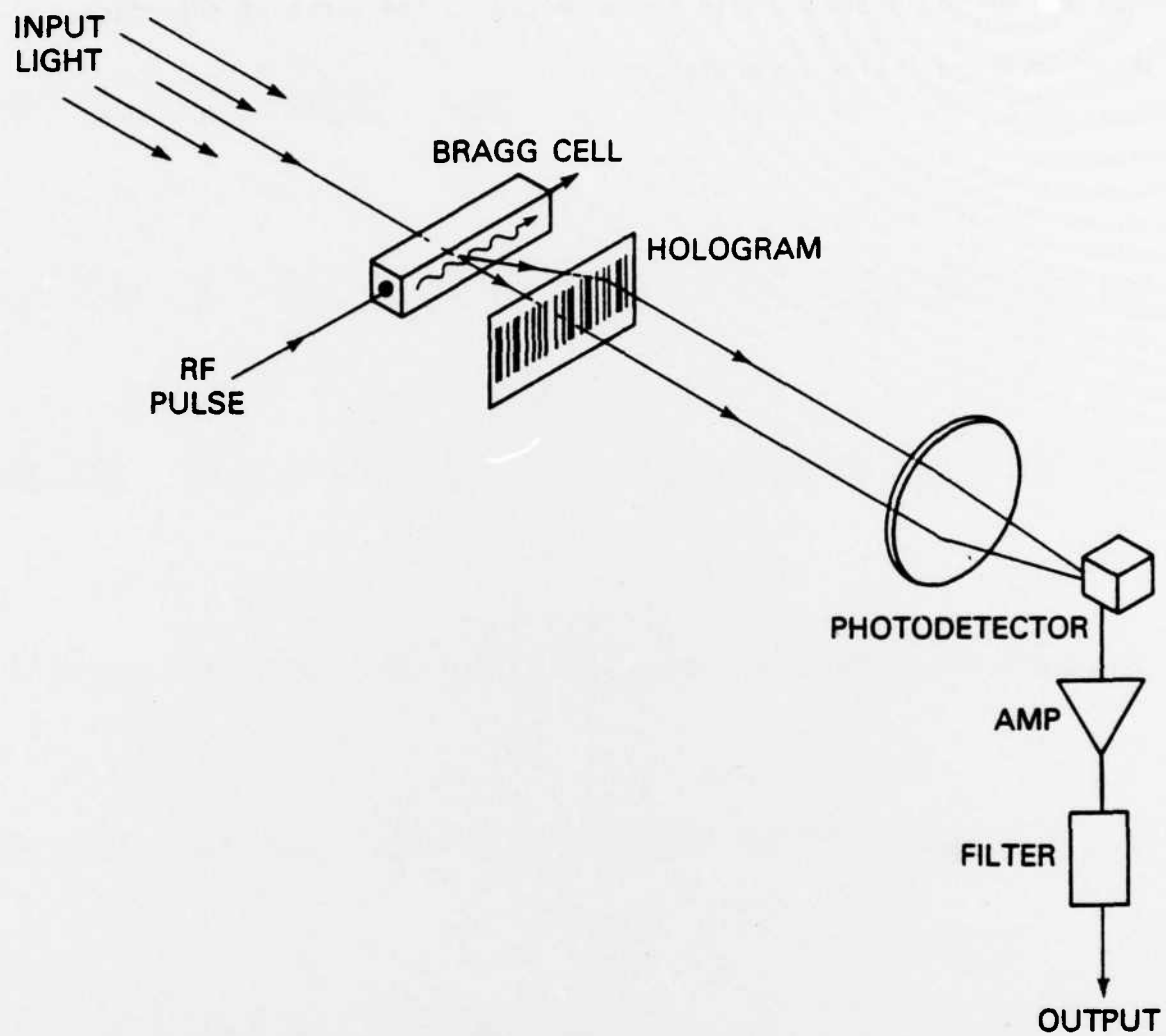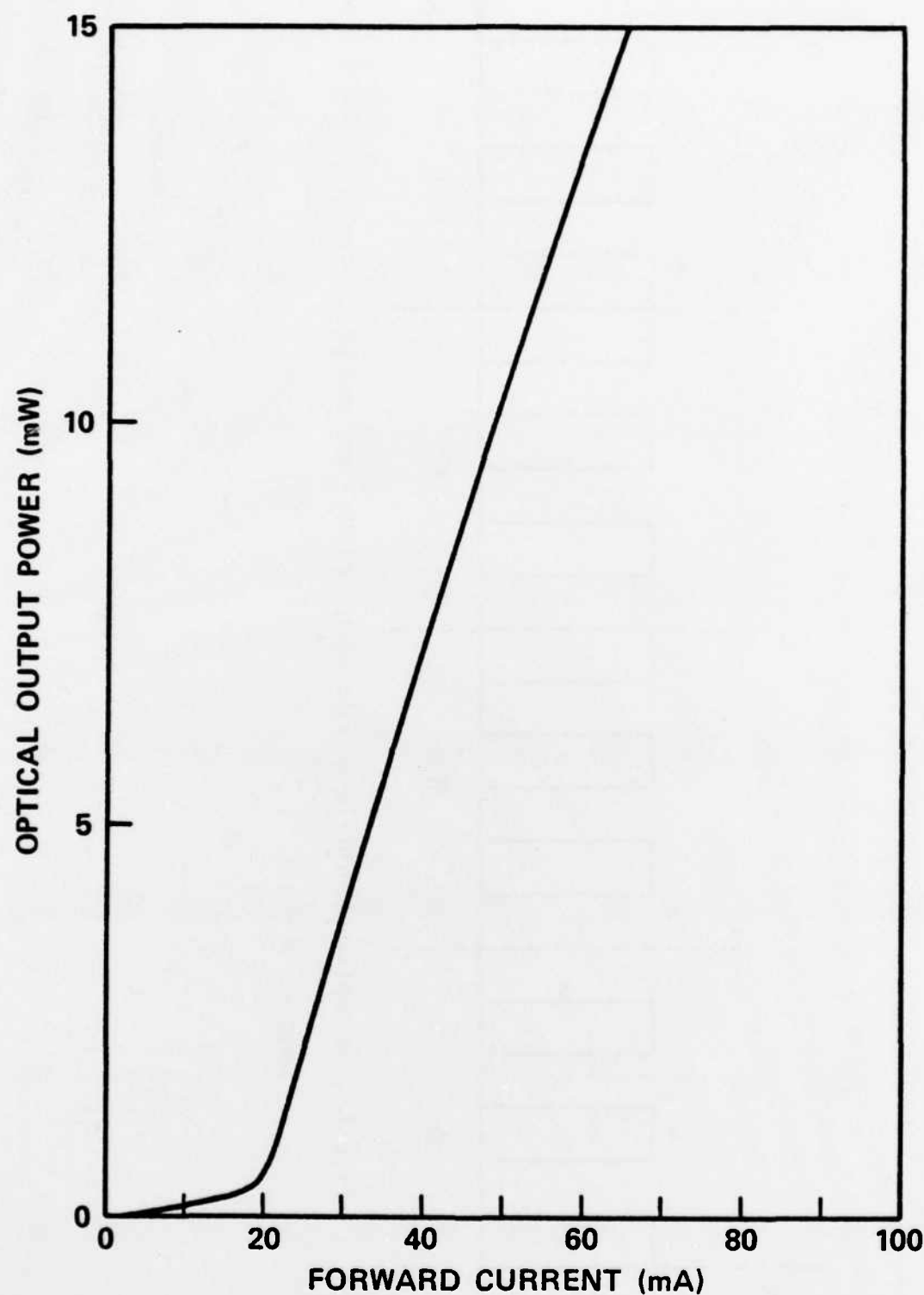
Fig. 1.   The optical pulse compressor arrangement.

12

Fig. 2. A typical diode laser output power versus the operating current (Mitsubishi Model ML-5308).
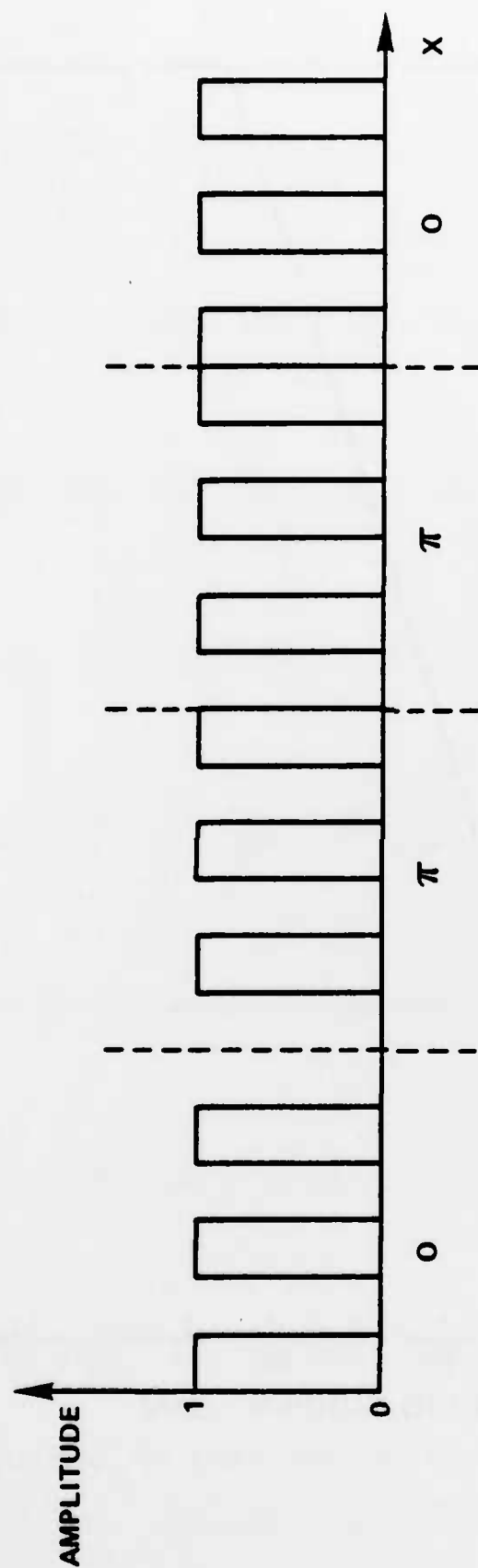
Fig. 3. The amplitude profile of a holographically - encoded phase - code sequence 0 π π 0.

14
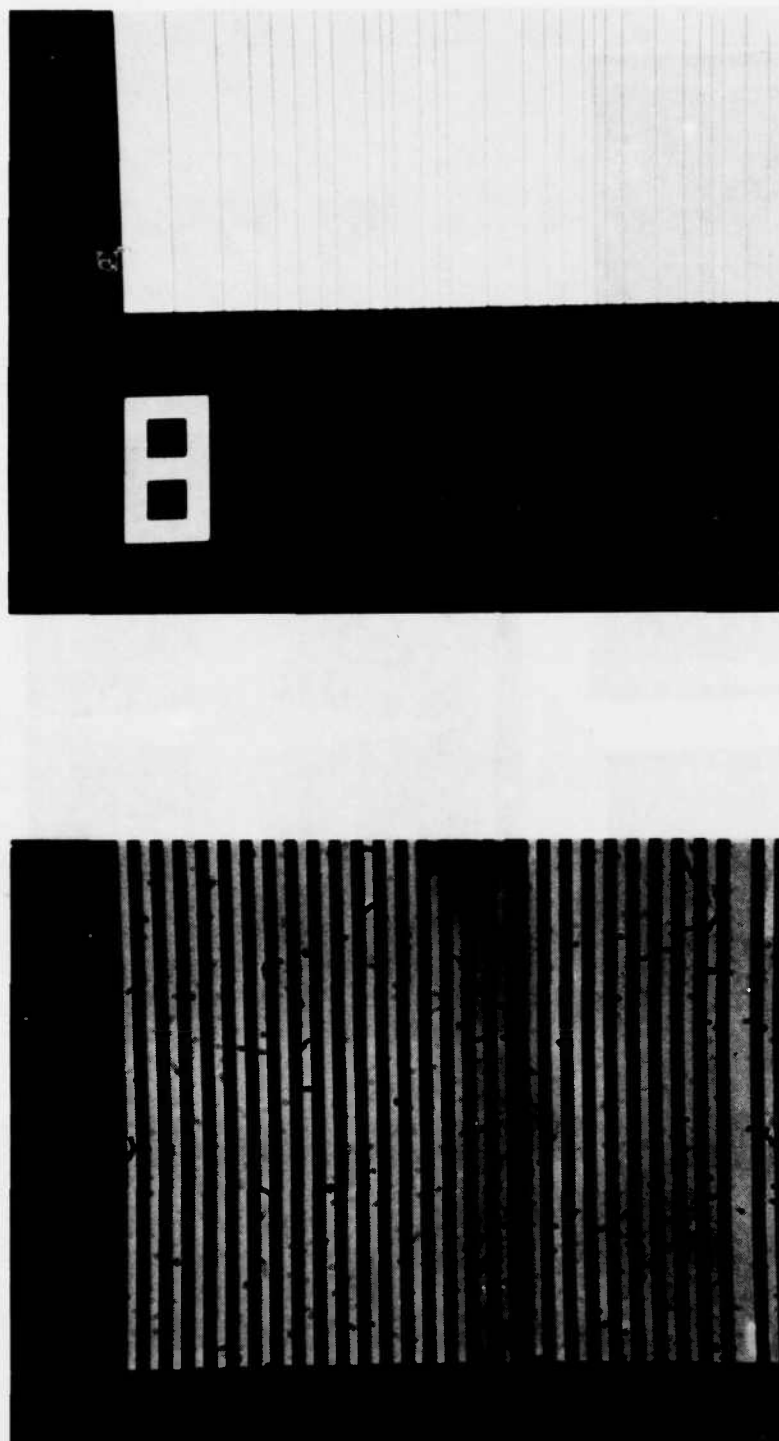
Fig. 4. Computer-generated holograms. The left picture shows the amplitude grating as illustrated by Fig. 3. The picture on the right shows part of the 511-bit pseudorandom code, where the smallest width of the bands is one bit length.
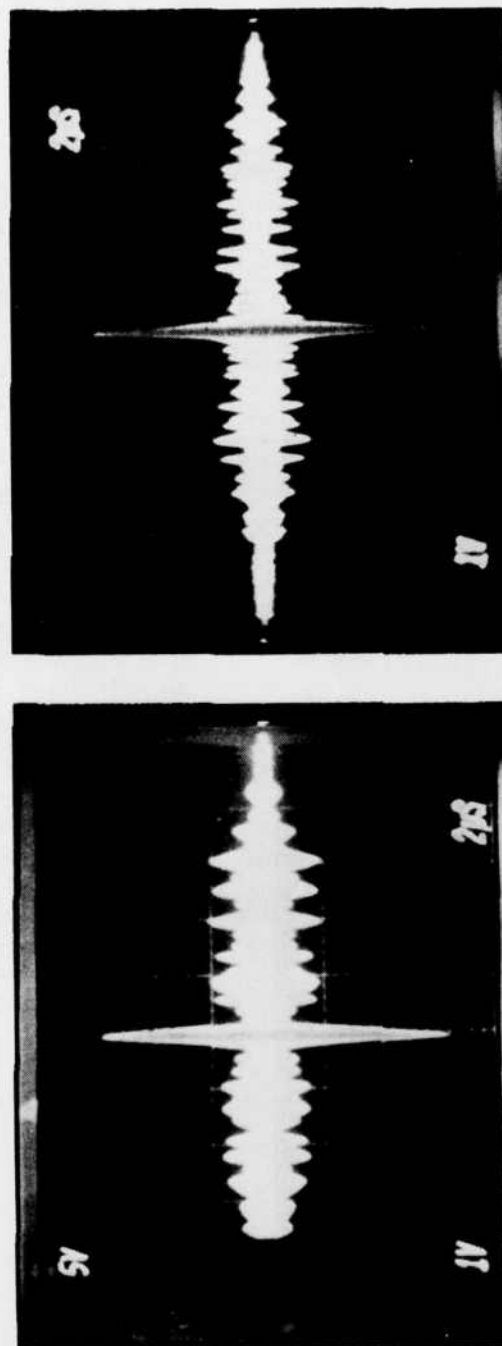
15
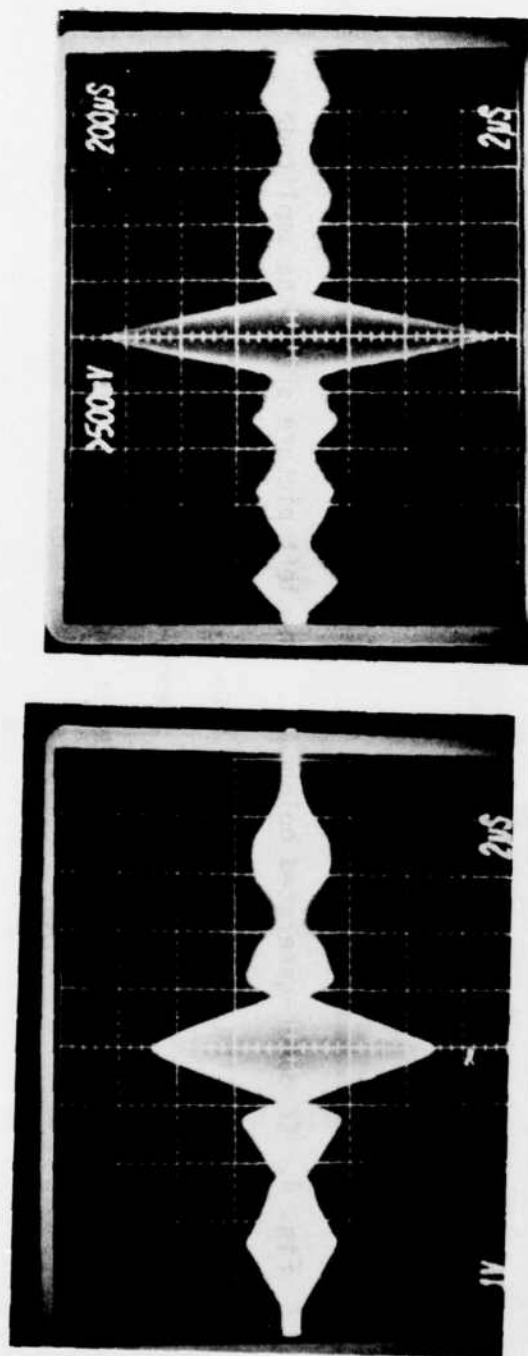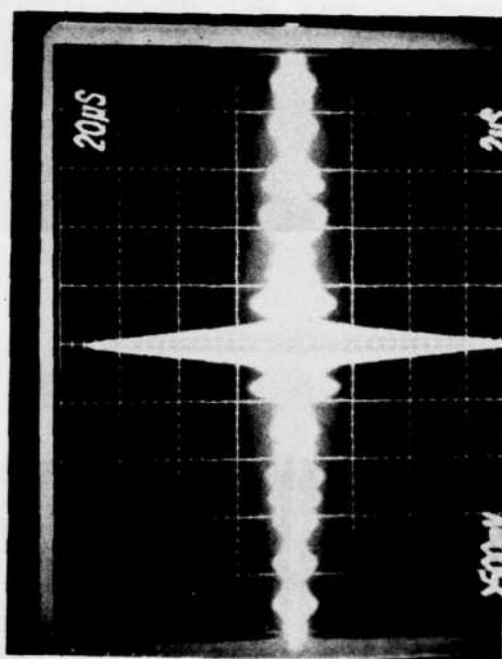
Fig. 5. Experimental results of the pulse compressor with Barker codes of 4 bits (a), 7 bits (b) and 13 bits (c). The light source is a He-Ne laser.

(a)

(b)

Fig. 6. Compressed pulses of pseudorandom codes of lengths 31 bits (a) and

63 bits) (b). He-Ne laser source.

17

(a)

(b)
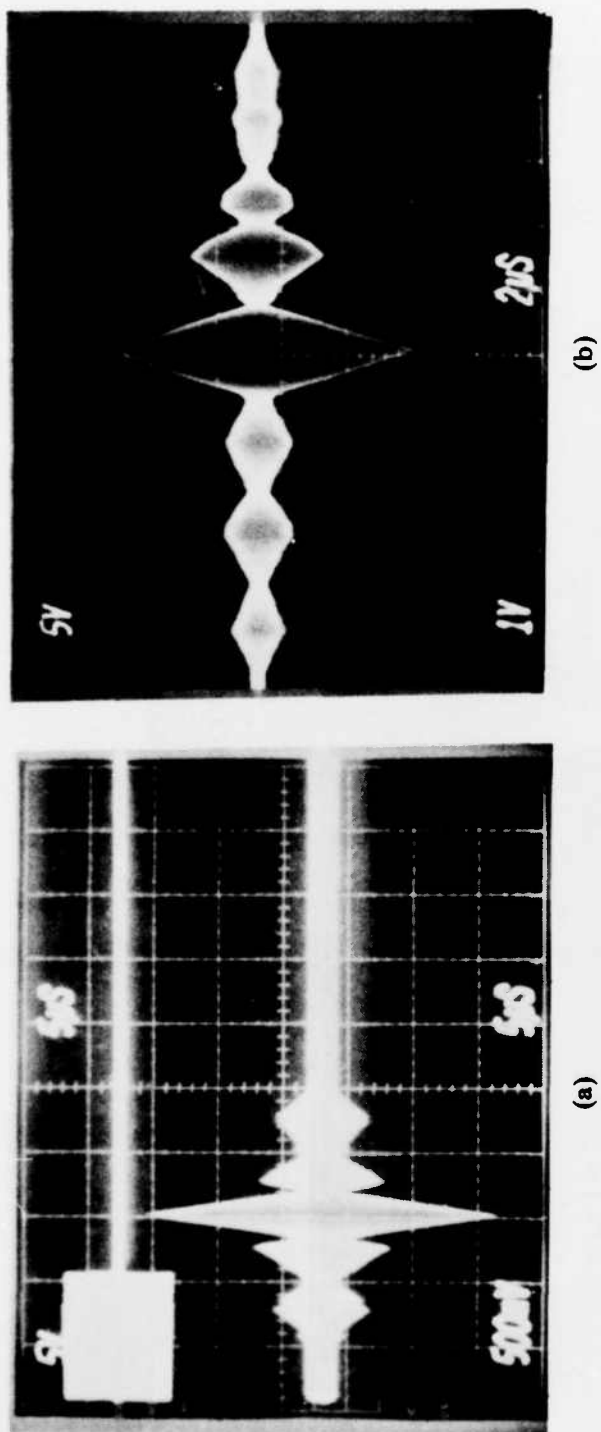
Fig. 7. Experimental Results with the Mitsubishi diode laser set at 7 mW output. (a), 4-bit Barker code: the upper trace shows the encoded RF pulse of 10 μsec duration. The lower trace gives the correlation of the coded pulse (b) compressed pulse of a 7-bit Barker code.
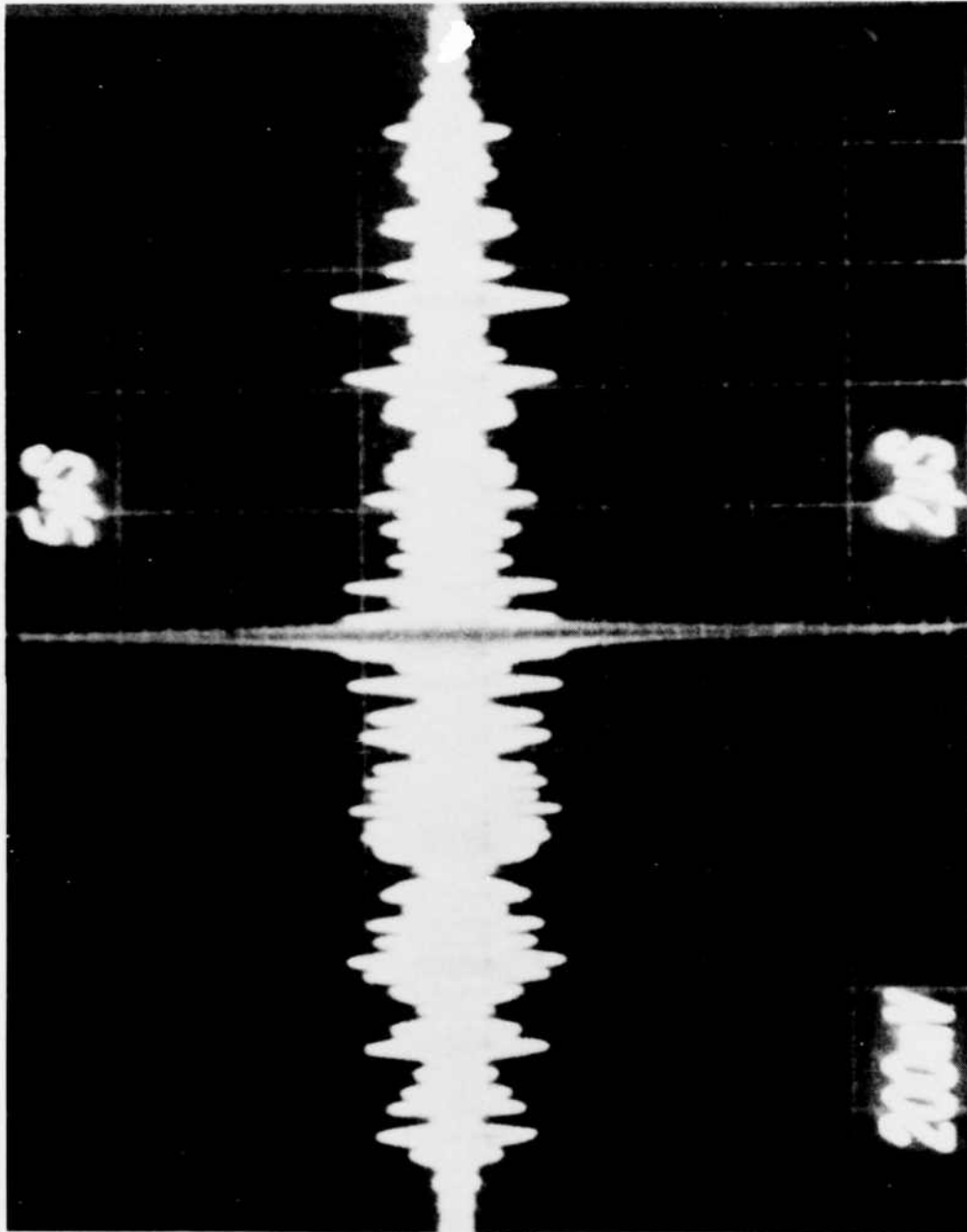
18

Fig. 8. Pulse compression result of a 127-bit pseudorandom code, with diode laser as the light source.
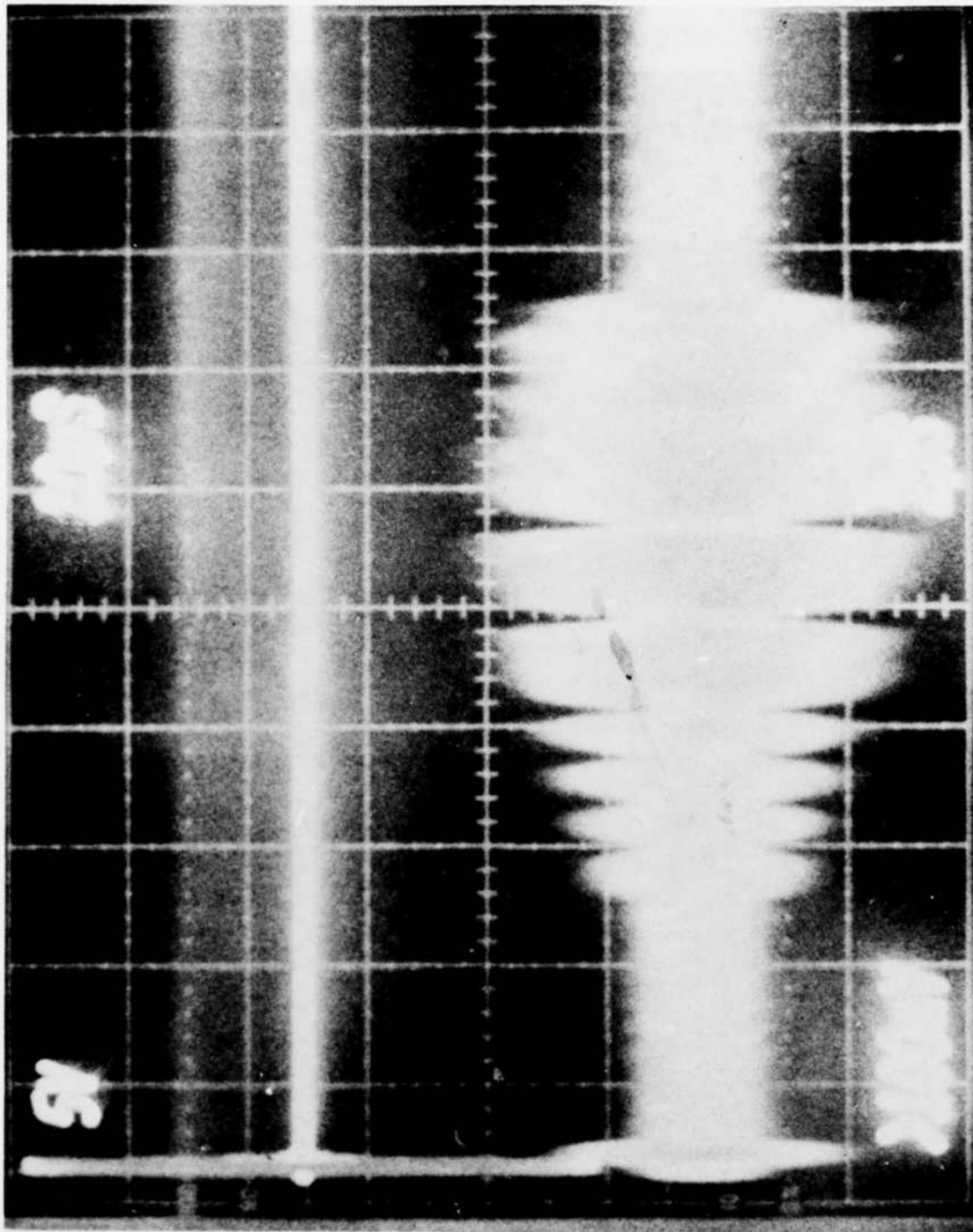
Fig. 9. Time-reversed readout of the 13-bit Barker code. The upper trace
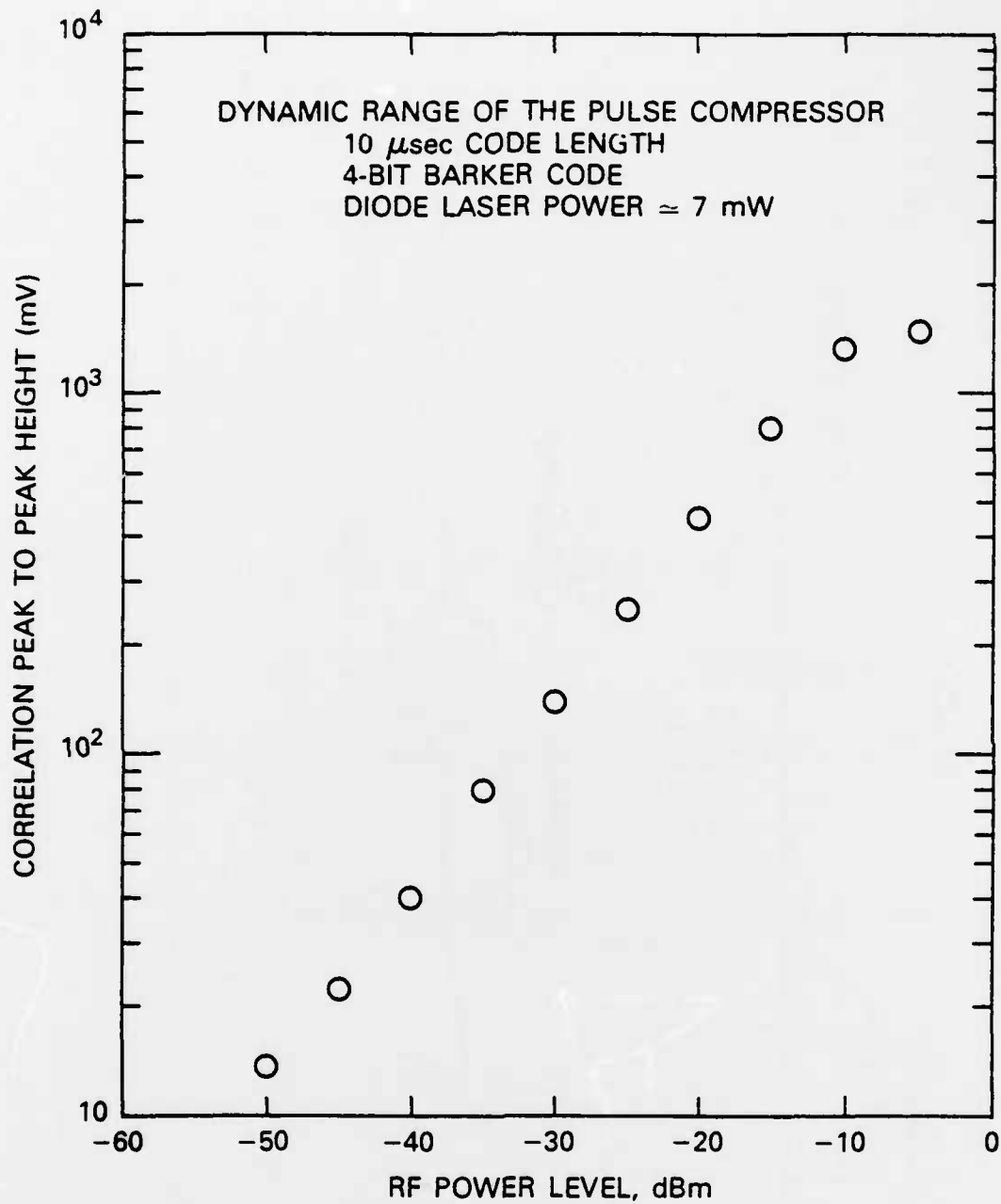shows the finite pulse used to simulate the delta function.

20

Fig. 10. Dynamic range measurement for the pulse compressor in the case of 4-bit Barker code. 40 dB is noted.
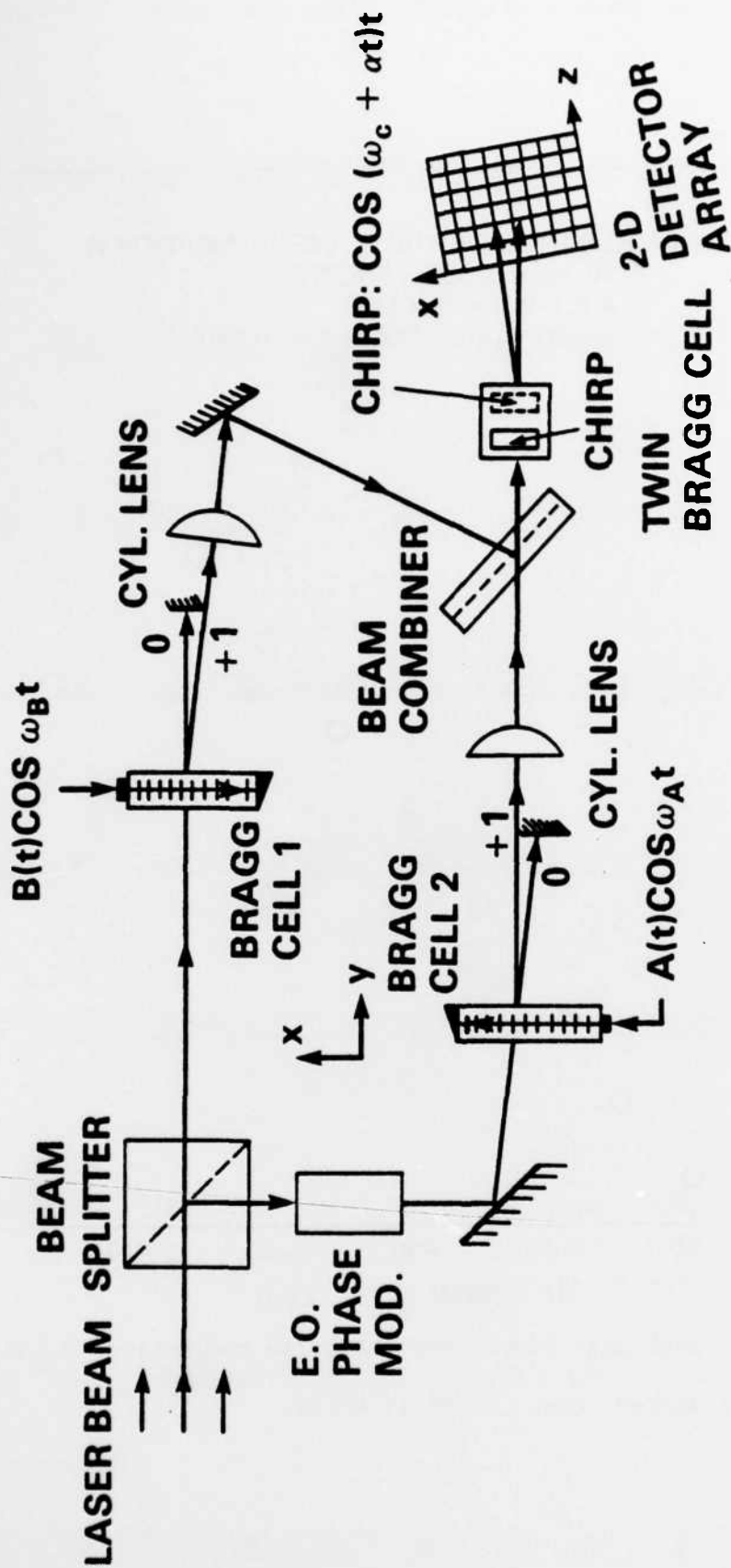
21

Fig. 11. Optical processor scheme for Doppler frequency shift measurement.

REFERENCES

1. F. C. Farnett, T. B. Howard and G. H. Stevens, Ch. 20 of "Radar Handbook", M.I. Skolnik (ed.), McGraw-Hill Book Co., New York, 1970.

2. Introduction to Radar Systems, M. I. Skolnik, pp. 428-430, McGraw-Hill Book Co., New York, 1980.

3. B. D. Cook and F. Ingenito, "Ultrasonic transducer configuration for producing a phase grating of nearly uniform strength," Proc. IEEE. 56, 871, (1968).

END

FILMED

9-83

DTIC